A novel approach to estimate temperature effects on strut loads in braced excavation

Ming Wu[1] , Xin Liu[1], Tangdai Xia[2], Xueyu Geng [3]

1 Department of Geological Engineering, Chang'an University, Xi'an 710054,Shaanxi,China

2 College of Civil Engineering and Architecture, Zhejiang University 866Yuhangtang Road, West Lake District, Hangzhou 310058, China P.R.;

[3] School of Engineering, University of Warwick, Coventry, UK, CV4 7AL

Corresponding author: Dr. Ming Wu. Associate Professor, Department of Geological Engineering, Chang'an University, Xi'an 710054,Shaanxi,China. e_mail:d05wuming@zju.edu.cn ; Tel:+8618092661560.

Co_ author: Dr. Xin Liu, Lecturer, email:liuxinsunny08@126.com

Co_ author: Prof. Tangdai Xia , email :xtd@zju.edu.cn

Nomenclature

A_c = end area of the strut (m^2);

B = beam width (m);

b_0 = beam computing width (m);

β = an empirical index equal to or higher than zero (dimensionless);

D = horizontal strut spacing or pile spacing according excavation design details (m);

E = elastic modulus of beam (MPa);

E_c = elastic modulus of strut (MPa);

α = coefficient of thermal expansion (1/°C);

E_s = elastic modulus of soil (MPa);

H = depth of excavation (m);

H_i = height from the top of excavation to the axis of the *i*-th-level strut (m);

H_n = height from the top of excavation to the axis of the *n*-th-level strut (m);

h_0 = height above the first-level strut (m);

h_i = height between the i-th- and (i+1)-th-level strut (m);

h_{i-1} = height between the (i–1)-th- and i-th-level strut (m);

h_{n-1} = height between the (n-1)-th- and n-th-level strut (m);

h_n = height between the bottom of excavation and n-th-level strut (m);

I =moment of inertia for beam section (m^4);

I_c = influence factor for foundation shape and point of analysis, i.e., corner versus center of footing (dimensionless);

k_h= horizontal coefficient of subgrade reaction (kN/m^3);

L = length of strut (m);

m= parameter of subgrade reaction(kN/m^4);

N_i^0, N_{n-1}^0 and N_n^0 = thermal strut loads at the i-th-level, the (n-1)-th-level and the n-th-level with ends perfectly fixed, respectively (kN);

N_n^1, N_n^2, $N_n^{j-1}$and N_n^j= temperature loads of the n-th-level strut under the first ,the second, the (j-1)-th and the j-th iteration computation, respectively (kN);

N_i^T , $N_{n-1}^T$and N_n^T= temperature-induced strut loads at the i-th-level , the(n-1)-th-level and the n-th-level strut, respectively (kN);

Q = strut load per width (kN/m);

s = vertical strut spacing (m);

ΔT = temperature change (°C);

υ = Poisson's ratio of the soil (dimensionless);

Y_n^0, Y_n^1 and Y_n^j = strut displacement at the n-th-level by N_n^0, under the 1-th and the j-th iteration computation, respectively (m);

Y_i= displacement of strut at the i-th-level strut (m);

Y_n = displacement of strut at the n-th-level strut (m);

y_i = wall deformation located at $h_i/2$ below the i-th-level strut (m);

y_{n-1} and y_{n-2} = wall deformation located at $h_{n-1}/2$ above the n-th-level strut and at $h_{n-2}/2$ above the (n-1)-th-level strut, respectively (m);

y = horizontal deformation of beams (m);

z = depth of sheet pile (m);

i,j,n= variables on defining the number of strut level or during computing process (dimensionless).

Abstract:

In deep excavation designs, strut loads play a key role to ensure excavation safety. During the construction, temperature fluctuation inevitably leads to a variation in strut loads. Therefore, how to quantitatively estimate the effects of temperature on strut loads is a matter of concern. In this note, the incremental changes in wall deflection due to temperature fluctuation were assumed to be piecewise linear. Based on the BEF model, a novel approach that accounts for the variation in temperature-induced strut loads at all levels was established. This model was further calibrated against a reported case study for a more precise predictive performance.

Keywords: Braced excavation, retaining wall, multilevel struts, temperature effects, strut loads

1. Introduction

For deep excavation design, apparent earth pressure diagrams are often employed to determine the maximum potential loads on struts. However, the apparent earth pressure consists of all contributing loading, including temperature-induced loads in struts. As excavations are becoming deeper and larger nowadays, excavation designs can be more reliable and inexpensive by separating loading component and quantitatively estimating the magnitude of thermal loads. It was reported that ignoring temperature effects on strut loads affected the safety of deep excavation by overstressing the struts or failing the supporting system (Arboleda-Monsalve, 2014; Bono et al., 1992; Powrie and Batten, 2000; Zhang and Yao, 2005). Thus, codes and design guidance (Twine and Roscoe, 1997; Gaba et al., 2003; CCEMS, 1997) suggested several approaches to consider temperature effects on strut loads for safety and economic design. Particularly, codes (CCEMS, 1997) stipulated that the thermal loads accounting for 10% the total strut load (when the strut length exceeds 40 m) was expected in an excavation design.

In last decades , many researchers and practitioners have documented a significant amount of cases in related to temperature effects on strut loads (Chapman et al., 1972; Twine and Roscoe, 1997; Kumagai et al., 1999;Richards et al., 1999; Boone and Crawford, 2000;

Hashash et al., 2003; Osborne et al., 2007; Chambers et al., 2016). By analyzing monitoring datum offered by above literatures, the changes of thermal loads in struts vary from approximately 65kN to 19kN per 1 °C as to different retained soil and various types of retaining structures across almost the world. It is still very challenging to estimate the temperature-induced loads by merely an empirical efficient from the empirical expression suggested by design guide Ciria C580 (Twine and Roscoe, 1997; Powrie and Batten ,2000; Gaba et al., 2003). Moreover, it was reported that temperature-induced strut loads account for a significant proportion of the total load , which is almost as high as nearly 37% of the total load (Richards et al., 1999). This finding prove the code (CCEMS, 1997) has been overestimated the safety of the xxxxx….which may lead to serious failure of the infrastructure. Thus, it is of important to estimate the temperature-induced strut loads more accurately.

To asset temperature effects on retaing structure, several numerical studies were conducted by Kumagai et al. (1999), Boone and Crwaford (2000) and Hashash (2003). the findings show that numerical tool is accurate to estimate thermal loads in strut. Nevertheless, as to a majority of engineers and practioners, empircal approaches are still more convinient in certain occasion. Thus, mainly three kinds of approaches (Endo and Kawasaki ,1963;Chapman et al., 1972; Twine and Roscoe, 1997; Boone and Crawford, 2000) were proposed to calcaulted temprature-induced loads in struts. (i) Endo and Kawasaki (1963)[as citied in (Boone and Crawford, 2000)] studied the relationships between thermal load and the elastic properties of the retained soil and proposed an equation by taking the retained soil as springs. However, the equation does not take the effect of strut spacing into account. (ii) By considering the lateral deformation of large sections of the retaining wall analogous to elastic settlement of a rectangular foundation and then using the Boussinesq solution (Terzaghi et al, 1996), an empirical expression(Chapman et al., 1972) was derived and later employed to estimate the thermal loads in several reported cases (Hashash et al., 2003; Boone and Crawford, 2000). (iii) Furthermore, Twine and Roscoe(1997) and Gaba et al (2003) suggested that temperature-induced loads can be estimated by the emprical expression, consisting of the degree of end restraint provided by the wall and the retainded soil and the thermal loads ocurred in strut with tow ends fixed. The degree of end restraint of the strut are recommanded to be 70% for stiff walls in stiff ground and 40% for flexible walls in stiff ground. A number of cases (Batten et al., 1999;Richards et al., 1999; Powrie and Batten, 2000;Chambers et al., 2016) were analyzed by using the the degree of restiant because of its simplicity. One of the findings shows that the degree of end restraint of the strut are as small as nearly 34% (Richards et al., 1999), which made the expression less desirable（意思说这样的结果说明 Twine and Roscoe(1997)的经验公式不太让人满意）. Additionally, it is very difficulty to select the degree of end restraint of the strut properly when deep excavation occurred at totally new soil deposites and without any experiences on parameter selection accumlated in advance.

However, these empirical approaches neglected the interaction between the temperature-induced strut loads and the deformation of retained soil (i.e., mathematically consider the temperature-induced strut loads to be a constant value). In this paper, the interaction is implemented by the combination of several equations and an iteration process indicated by a calculation flow chart. Furthermore, the Boussinesq solution assumes that a concentrated load is applied at a point on the surface of an elastic half-space mass. Obviously, the assumption cannot be strictly applied to meet the boundary conditions of excavation engineering, whereas the Mindlin solution (Mindlin, 1936; Mu et al., 2012) and the beam-on-elastic-foundation (BEF) approach are more appropriate. The BEF approach (He et al., 2017; Li et al., 2009; Poulos and Davis, 1980; Liang et al., 2017) deduced from the Winkler model is more practical when analyzing the interactions between soil and structure. Most importantly, these empirical approaches cannot identify the temperature-induced strut loads carried in different level strut if the details of bracing systems and the retained soil are the same. By assuming the deflection of wall as a piecewise linear function, the proposed approach can make it.

Therefore, a approach to combine the interaction process between the temperature-induced strut loads and the deformation of retained soil and the BEF theory is introduced to estimate the temperature-induced strut loads in different level strut. The proposed approach is convenient for use in the design and assessment of deep braced excavations

2. Excavation Analysis using Beam in Elastic Foundation Approach

Winkler's model has been widely used in the analysis of soil–structure interactions. The soil mass in this theory assumed as a series of individual soil springs and defines the stress–strain response of the soil–structure interaction as the foundation reaction coefficient. In excavation designs, the BEF approach can be used for the stress and deformation analysis of the retaining wall. As shown in Fig. 1, the retaining wall is simplified as a beam on elastic foundation. The retained soil is composed of a series of soil springs at both sides of the wall, whereas the struts are springs of different rigidities. The governing equation can be expressed as follows(Poulos and Davis,1980; Xiao et al., 2003):

$$EI\frac{\mathrm{d}^4 y}{\mathrm{d}z^4} + k_h \cdot y \cdot b_0 = 0 \tag{1}$$

where E = elastic modulus of the beams; I = moment of inertia of the beam section; y= the horizontal deformation of the beams; b_0= the beam computing width; k_h = the horizontal coefficient of the subgrade reaction. In deep excavation, k_h increases with depth, and it is estimated using Eq. (2) (Poulos and Davis, 1980; Xiao et al., 2003):

$$k_h = m \cdot z^{\beta} \tag{2}$$

where β= an empirical index equal to or greater than zero; m= the parameter of the subgrade reaction (i.e., when β = 1, the dimension for kN/m^4); and z = the depth of the sheet pile. Based on the soil layer, β can be valued as 0, 0.5, or 1. Notably, β = 1 is mostly used in China based on extensive engineering experience.

3. Temperature Effects on Strut Loads

In response to temperature fluctuation, strut loads change accordingly. If the strut ends are perfectly fixed without horizontal displacement, the variation of strut load only depends on the temperature change and is expressed as follows (Beer et al, 2012):

$$N_i^0 = \alpha \cdot \Delta T \cdot E_c \cdot A_c \tag{3}$$

where α = the coefficient of thermal expansion; ΔT = the temperature change (degree); A_c = the end area of the strut; E_c = the elastic modulus of strut; and i=the number of the i-th-level strut. In fact, the strut loads are resisted by the soil mass within a certain range behind the wall. Terzaghi et al.(1996), reported that the influence zone is rectangular, and the horizontal distance is close to pile spacing D (see Fig. 2 for terminology). The vertical distance is the sum of half of spacing *h* between the upper- and lower –level struts as shown in Fig. 2. In this paper, to consider wale strengthening effects on retaining wall, *D* is defined as the horizontal spacing of struts for retaining wall with walls, or pile spacing for that without walls. As shown in Fig. 2, the soil mass behind the walls was simplified as a series of soil springs. When the strut loads change due to temperature effects, producing a deflection of the wall, the soil springs behind the wall will deform correspondingly. Simultaneously, the deformation of soil springs induces a variation in the restraint conditions of the strut-end, influencing the strut loads in turn. Finally, the equilibrium between strut loads and deformation of soil springs will be achieved.

4. Model for Multilevel Struts Loads

As shown in Fig. 3(a), wall deflections are produced like curve 1 due to excavation, and the wall deflection will slightly change to curve 2 owing to temperature-induced strut loads. Therefore, the incremental changes in wall deflection induced by temperature fluctuation occur. The superposition principle can be applied to them. Hence, herein, we specifically focused on the incremental changes in wall deflection induced by temperature fluctuation, whose deflection shape was assumed as a piecewise linear function (as shown in Fig. 3(b) with magnification), i.e., in each influence zone, the shape of the incremental changes of wall deflection was conceived as a straight line. To validate this assumption, we introduced the only monitoring results (Chapman et al., 1972) recorded to investigate the relationship between temperature-induced strut loads and the corresponding wall deflection. According to Chapman et al.(1972), the strut load induced by temperature effects led to a wall deflection of 2 mm, ~0.13% of the excavation depth of 15 m. Compared to the excavation depth, the wall deflection induced by temperature effects is very small. Therefore, to some extent, the assumption is a brave attempt to investigate the topic, because no more effective measured results aim to serve the point. Luckily, the results reported in the next section obtained by the proposed approach show a good performance.

Fig. 4 shows that the temperature-induced loads at the i-th-level strut are resisted by the soil mass with depth in between $h_{i-1}/2$ and $h_i/2$. The horizontal strut displacement induced by temperature effects at the i-th level is Y_i, also equivalent to the incremental horizontal deflection of retaining wall at the strut level. The corresponding horizontal wall deflections for the upper $h_{i-1}/2$ and lower $h_i/2$ of the i-th level strut are y_{i-1} and y_i, respectively. Y_i, y_{i-1}, and y_i can be expressed using a linear equation in influence zone with the local coordinate system as shown in Fig. 4.

$$y = -\frac{2(Y_i - y_i)}{h_i} z + Y_i + (Y_i - y_i)\frac{h_{i-1}}{h_i} \tag{4}$$

The relationship among Y_i, y_{i-1}, and y_i can be expressed as follows:

$$y_{i-1} = y_i + \frac{(h_{i-1} + h_i)(Y_i - y_i)}{h_i} \tag{5}$$

Because wall deflection is resisted by soil springs behind the wall, according to the Winkler's model, for an infinitesimal dx at x in the local coordinate system of the i-th-level strut (see Fig. 4 for terminology), the temperature-induced strut load can be expressed as follows:

$$\mathrm{d}Q = k_h\, y\, \mathrm{d}z \tag{6}$$

By integrating Eq. (6),

$$Q = \int_0^{(h_i + h_{i-1})/2} k_h y \,\mathrm{d}\, z \tag{7}$$

where $k_h = m(z + H_i - \frac{h_{i-1}}{2})$is the horizontal subgrade reaction coefficient. By substituting k_h and Eq. (4) into Eq. (7), the temperature-induced strut load per width can be derived as follows:

$$Q = \int_0^{(h_i + h_{i-1})/2} m(z + H_i - \frac{h_{i-1}}{2})\left[-\frac{2(Y_i - y_i)}{h_i} z + Y_i + (Y_i - y_i)\frac{h_{i-1}}{h_i}\right] \mathrm{d}\, z \tag{8}$$

The temperature-induced strut load at the i-th-level is $N_i^T = D \times Q$. Here, the subscript in N_i^T indicates the temperature-induced load of the i-th-level strut. By integrating Eq. (8),

$$N_i = \frac{mD\left(h_i + h_{i-1}\right)\left[\left(Y_i + 2y_i\right)(h_i^2 - h_i h_{i-1}) + 6H_i h_i\left(Y_i + y_i\right) + \left(Y_i - y_i\right)(6H_i h_{i-1} - 2h_{i-1}^2)\right]}{24h_i} \tag{9}$$

Eq. (9) can be rewritten as follows:

$$Y_i = \frac{\dfrac{24N_i^T h_i}{m\left(h_i + h_{i-1}\right)D} - 2y_i\left(3H_i(h_i - h_{i-1}) + h_i^2 - h_i h_{i-1} + h_{i-1}^2\right)}{\left(h_i + h_{i-1}\right)\left(h_i + 6H_i - 2h_{i-1}\right)} \tag{10}$$

5. Approach for Calculation of Strut Loads at Bottom Level

Terzaghi et al. (1996) considered only the soil mass with half depth below the bottom-level strut when calculating apparent earth pressures. Here, for the *n*-th-level strut, a similar approach was used, i.e., the position where the wall horizontal displacement caused by temperature-related loads is equal to zero is located at $h_n/2$ (see Fig. 7 for terminology). Therefore, for an excavation with n-level struts, the temperature-induced strut load at the n-th-level is resisted by the soil mass within the range of upper $h_{n-1}/2$ and lower $h_n/2$ of the n-th-level strut. An approach to compute the temperature-induced strut loads for the *n*-th-level was established similarly to the *i*-th-level strut, as shown in the Appendix.

6. Computation Process

To implement the interactions induced by temperature effects between the retaining wall and soil, the following processes are specifically demonstrated by taking the example of the *n*-th-level strut. First, when struts were fixed at both the ends and underwent an increasing temperature change ΔT, the strut temperature load is equal to N_n^0(computed using Eq. (3)). Herein, subscript n refers to the n-th-level strut, and superscript 0 indicates the variable of the iteration processes for the struts at the same level (initial temperature loads). However, after exerting the strut temperature loads N_n^0, the soil within influence zone will deform correspondingly, and the displacement of retaining wall Y_n^0can be computed using Eq. (18) shown in appendix. According to displacement compatibility, the strut supporting the influence zone will elongate by a total amount of 2 Y_n^0(tow ends), producing an variation of strut temperature loads:

$$\Delta N_n^0 = \frac{A_c \cdot E_c}{L} \cdot 2Y_n^0 \tag{11}$$

Then, strut temperature loads N_n^0 decrease to N_n^1:

$$N_n^1 = N_n^0 - \frac{A_c \cdot E_c}{L} \cdot 2Y_n^0 \tag{12}$$

The strut temperature loads are now updated to N_n^1; once again, for soil exerted by a new thermal load N_n^1 within the influence zone, Y_n^1 can be obtained using Eq. (18) shown in the Appendix. Then, N_n^2 can be obtained using Eq. (12). By repeating the above processes till the relative error between N_n^j and N_n^{j+1} is very small (such as less than 10%), the average is obtained as the temperature-induced strut load. Several steps as shown following are suggested in detail to implement the above process, simultaneously presented in flow chart Fig 6.

Step 1. Calculate the initial temperature loads. After inputting basic parameters, calculate initial temperature loads N_n^0 in the n-th-level strut by Eq.(3).

Step 2. Calculate the deformation in retained soil. By substituting N_n^0 into Eq.(18) in the Appendix and Y_n^0, the displacement of the the *n*-th-level strut is obtained, which is equal to the deformation of the retained soil according to the displacement compatibility.

Step 3. Calculate the thermal loads in the strut. Calculate the thermal loads of the *n*-th-level strut N_n^1 by substituting Y_n^0 into Eq. (12).

Setp 4. Judge whether or not $N_n^j \geq 0$. If yes (Case 1), then setting j=j+1 and referring back to step 2 to calculate Y_n^{j+1} by substituting N_n^j into Eq. (18) in the Appendix. The above iterative loop runs from step 2 to step 3 until the relative error between two consecutive variables is less than a given value, such as 15% or 10%.

Step 5. For the case of the negative thermal load in the strut. If N_n^j <0 (Case 2), this case often occurs in the softer ground and means the retained soil produced an excessive deformation after bearing N_n^{j-1}. Correspondingly, this deformation let the strut elongated too much and the negative thermal loads cannot certainly be produced in reality. For case 2, to crack the matter, two substeps are shown as following. Judging whether or not $N_n^{j-1}$is approximately equal to zero. (i) If yes, the thermal load N_n^T can be set to zero and outputting results. (ii) If not, Reducing N_n^0 in a manner, such as N_n^0= N_n^0-0.1 N_n^0 or other similar ways.

And the reducing N_n^0 is given to N_n^{j+1} and then go to step 2, i.e. N_n^{j+1} is given to N_n^T of Eq. (18) in the Appendix. Repeating the iteration loop from step 2 to step 3 until the equilibrium is achieved.

Herein, the key point in the processes is to achieve the equilibrium between the force offered by the retained soil and the released thermal load remained in the strut. Specially, the temperature-induced load is view as zero if N_n^{j-1} is nearly reducing to zero and the equilibrium is still not achieved yet. Actually, this means the strut is nearly release to the free condition because of the retained soil with lower stiffness.

Step 6. Output results and prepare the input parameters for level n-1 strut. Finally, the equilibrium among soil, retaining wall, and strut is achieved, which are unfortunately not involved in the papers(Endo and Kawasaki ,1963;Chapman et al., 1972; Boone and Crawford, 2000; Gaba et al., 2003)and presented graphically in Figures 7-9. In addition, after the temperature-induced strut load N_n^T and the corresponding displacement Y_n of the n-th-level strut was obtained, y_{n-1}(see Fig. 5 for the term) computed by substituting Y_n into Eq.(15) in the Appendix was employed for the calculation of the (n-1)-th-level strut. As shown in Fig.6, the calculation processes start from the n-th-level strut and are repeated in the next strut level until the first-level strut is achieved. The following three cases were calculated according to above processes and Computer program source codes written by Maple language are provided as Supplementary material.

7. Example of Applications

Because studies on the topic are very few, only one paper (Chapman et al., 1972) monitored the relationship between temperature-induced strut loads and the corresponding wall deflection and provided the detailed excavation design parameters. Therefore, the practical excavation in paper (Chapman et al., 1972) was selected to validate the proposed approach. The excavation had a length of 41.3m, a width of 25.5 m, and a depth of 12.7-15.2m. The sheet-pile wall was made up of V-50 steel piles of W18×50 and a wood lagging with a thickness of 7.6 cm. The maximum pile center spacing was 2.8 m. A-36 steel of HP14×73 was used in cross-lot braces. According to the model proposed in this paper, the excavation depth was 15.2 m. Besides, $h_1 = 5.58$ m, $H_1 = 3.1$ m, $h_2 = 6.51$ m, $H_2 = 8.68$ m, $m = 1734$ kN/m^4, strut length $L = 25$ m, cross-area of strut $A_c = 0.014$ m^2, the coefficient of thermal expansion α= 1.17E-5, the elastic modulus of steel struts E_c = 2.06E8 kN/m^2, cross-lot brace spacing D = 5.5-m, and ΔT = 22.2 °C (40 °F).

The computed results of strut load at the second- and first-levels using the proposed approach are shown in Figs. 7 and 8, respectively, where the iterative processes shed light on the interactions between the retaining wall and retained soil. The processes are shown with the data in a clockwise circulation. A smaller deflection of the retaining wall exhibits larger strut loads; therefore, the restraint conditions of strut ends are very important to estimate the temperature-induced loads; i.e., the stiffness of retained earth directly affects the temperature effects on strut loads. With the criterion of relative (2% in this case) errors as mentioned above, for the second- and first-level struts, the temperature-induced strut loads (average values) are 482 kN and 404 kN, about 38% and 35% higher than the measured values, respectively.

Fig. 9 shows that the convergence occurs in a relatively few iterations during the computing processes, converging to 480 kN and 404 kN as for the second- and first-level struts, respectively. For engineering design, the computing processes are stopped intentionally when matching the relative error proposed above. As shown in Fig. 10, the iteration numbers are 7 and 4 for the second- and first-level struts, respectively, and are quite few for computer programs to calculate.

8. Comparison with other approaches

8.1 Validation with case 1

As shown in Fig. 10, the measured variations for temperature-induced strut loads at the first- and second-levels are 300 kN and 350 kN, respectively, equivalent to 41% and 47% of the initial temperature load (738 kN for a strut with perfectly fixed-ends), respectively. The measured values for the total strut loads at the fist-and second-levels are about 1150 kN and 1200 kN, respectively, and their variations for strut loads induced by temperature effects are about 26% and 29% of the value, respectively. This indicates that the strut loads induced by temperature effects cannot be ignored. The measured results show that the temperature effects on strut loads are more significant at the lower level than at the upper level. This phenomenon can be interpreted with the model illustrated in Figs. 3 and 4, where the lateral earth load resisted by the lower-level struts is larger than the upper-level struts. Thus, the retaining wall supported by lower-level struts is subjected to a larger resistance and a smaller deflection of the wall is produced when the temperature differences from the top to the bottom of excavation do not exceed 0 °C. This is same as the situation where the restraints are gradually released in smaller magnitudes at both the ends of struts. Therefore, the variation in strut loads caused by temperature effects is larger at a lower level when the temperature changes make no differences at each strut level.

To compare the proposed approach with others, Eq. 13(Liang et al., 2017;Huang et al., 2009; Vesic, 1961) was used to relate E_s and υ with k_h, because the previous approaches (Chapman et al., 1972; Hashash et al., 2003; Boone and Crawford, 2000) used parameters E_s and υ based on Boussinesq solution, while the proposed approach with parameter k_h uses the beam on elastic foundation theory.

$$k_h = \frac{0.65 \cdot E_s}{1-\upsilon^2} \cdot \left(\frac{B^4 \cdot E_s}{E \cdot I} \right)^{\frac{1}{12}} \tag{13}$$

where E_s = the modulus of elasticity of the soil; υ= the Poisson's ratio of the soil; B = the beam width; E = the modulus of elasticity of the beam; and I = the moment of inertia for beam section. Using Eqs. (13) and (2) (i.e., β = 1), m ≈ 1734 kN/m^4 or 8498 kN/m^4 at the second- and first-level struts, respectively. The process on obtaining the parameters is provided as Supplementary material.

Table 1 compares the prediction between the proposed approach and others reported in literature. The results from Boone and Crawford (2000) can not be used to calculate the temperature-induced strut loads at every level essentially because no displacement compatibility is essentiallly appled to the adjacent struts. So, both Chapman et al.(1972) and Boone and Crawford (2000) failed to distinguish the temperature-induced strut loads at every level. As the influence factor for foundation shape (i.e., I_c) decreases, the computed results of Boone and Crawford (2000) approach increase. However, for this practical project (Chapman et al., 1972), I_c is equal to 1.5, and by just considering different struts arrangement the computed result is about 220 kN for the second-level strut and 216 kN for the first-level strut ,respectively, less than the measured value. The computed results from Chapman et al.(1972)approach provide a satisfying prediction with the average of plate test modulus (E_s = 24 MPa), whereas the computed results become unreasonable large with back-analysis modulus (E_s = 137 MPa). In addition, the results from Chapman et al.(1972) show that the computed temperature-induced loads in the first-level strut provide larger safety margin accounting for 27% of the measured value, whereas safety margin for the second-level strut accounts for 9% of the measured value. It is not safe enough for the lower level strut while the proposed approach offer a proper safety margin at least accounting for 34% the measured value. It can be seen in the Table 1 that the maximum degree of the measured value is 47%. The ground behind the retained wall can be classified as stiff soil and the retained wall is composed of soil mixed wall (Chapman et al., 1972). This correspond to the situation of *flexible wall in stiff soil* and accordingly lead to select the degree of restraint of 40% (Gaba et al., 2003) which cannot cover the measured value (41% and 47%). The degree of restraint by the proposed approach is about 65%, which is within the range of the recommended value(Gaba et al., 2003) and desirably cover the degree of restraint.

In comparison, Boone and Crawford(2000)approaches offer an unsafe estimation of temperature effects on strut loads. Both Chapman et al.(1972) and the proposed approach offer a conservative prediction. the predicted values obtained from the proposed approach are more reasonable as they offer a proper safety margin. In the above context, several factors that affect the computation processes include the structural forms, spacing and length of struts, overall rigidity of wall, and stiffness of the retained earth, i.e., deformation modulus of soil or coefficient of subgrade reaction. The parameter study will be performed in later section.

8.2 Validation with case 2

An deep excavation, generally 17m in depth, has been constructed in the ground conditions of Lambeth Group Sands and Clays in UK (Powrie and Batten, 2000). The retaining wall consists of 900mm dia. reinforced concrete hard piles and 700 mm dia. weaker concrete piles. The tow level struts were fabricated from 1067 mm dia.×14.3 mm thick tubular-section steel and spanned 26.7 m (free distance 24.1 m) between the secant pile retaining walls. A detail monitoring program was conducted to record the excavation process, in which vibrating-wire strain gauges was employed to monitor the development of strut loads. In this case, the measured degree of restraint is about 52% for fist level strut and 63% for the second level strut, respectively.

Table 2 shows the comparison among different approaches. It can be seen that, for the first-level strut, a good agreement is presented by the proposed approach. Chapman et al (1972) also offer a good prediction for the second-level strut while Boone and Crawford offer an unconservative prediction. According to the excavation programs (Powrie and Batten, 2000; Batten et al.,1999) , the tow levels strut worked simultaneously for nearly 68 days (entire excavation sequence last about 300 days) and the second-level struts were deleted after that time. This means the second-level strut experienced less temperature fluctuation than the first-level strut. Thus, the authors believe that the degree of restraint maybe higher for the second-level strut as its usage lifespan last longer. So, the higher prediction by the proposed approach may be reasonable for this consideration. The average of the degree of restraint by the proposed approach is approximately 64% close to the value by Chapman et al (1972), which cover the average of the measured value (58%).

8.3. Validation with finite element model (FEM)

A symmetrical plain strain simulation was carried out to verify the effectiveness among the approaches using finite element software, Midas-GTS(2002). Fig. 11 shows the 2D element mesh and excavation dimensions. Soil behavior was modeled as a Mohr-Coulomb linear elastic perfectly plastic constitutive material with associated flow rule. To validate the extension of the approaches, elastic modulus of soil is intendedly selected to be 26 MPa, 60MPa and 260MPa, respectively,which appear to respond with clay, dense sand and a kind of stiffer soil in reality. For simplicity, the unit weight, friction angles, cohesion, and Poisson′s ratio of soil are 19kN/m^3,30°,0 kPa and 0.3 respectively and they keep constant during numerical analysis of the three cases. The wall of the excavation was supported by a 0.6-m-thick, 20-m-deep concrete diaphragm wall. The elastic modulus and Poisson′s ratio of the concrete diaphragm wall are 30GPa and 0.19, respectively. Tow struts with 609mm in diameter and 16mm in thickness were set up to limit lateral deformation of the wall, for which the elastic modulus , cross-section area, length and coefficient of thermal expansion are 200GPa, 0.015m^2, 20m (symmetrical problem) and 5×10^{-5}, respectively. Thus, the temperature-induced load in the steel strut with tow ends fixed is approximately 300kN when temperature increase of 20℃. In numerical analysis, the structural element beam is employed to simulate the wall and struts, the struts were imposed temperature increases immediately after excavation sequences finished. No interface element between retained soil and wall was considered.

Table 3 shows that the results from the proposed approach are closer to the numerical results than other approaches and are 2-3 times as large as the numerical results.

Boone’s (2000) approach perform better than Chapman’s (1972) approach though both approaches overestimate temperature-induced strut loads significantly. These overestimations in this case, which is quite opposite to the practical example in section 7, might be caused by the Boussinesq solution and neglecting the interaction. As shown in Table 3, for the case of E_S=26MPa, the thermal load in the first-level strut is about 1 kN, which indicates that the thermal load is released to the free conditions nearly. Obviously, the proposed approach can take it into consideration while others cannot.

9. Discussion with parameters

Fig. 12 shows the relationship between the temperature-induced strut loads that were normalized with respect to the thermal load with fixed ends (i.e., normalized thermal strut loads hereafter) and the stiffness of retained soil. The normalized thermal strut loads within the range from 0.5 to 0.8 increased with the stiffness of retained soil. This phenomenon can be readily interpreted using the soil-wall interaction process proposed in this paper. When the stiffness of the retained soil increases, the end-restraint effects are enhanced, and the temperature-induced strut loads increase. Fig. 12 also shows that the iteration number decreased with increasing soil stiffness. As shown in Figs. 13-15, the normalized thermal strut loads increased with the strut length, and the influence zone ($s \times D$) increased as well. In Fig. 16, the relationship between the strut stiffness and normalized thermal strut loads is shown by defining the strut stiffness as the product of elastic modulus of strut (E_c) and the strut crossing area (A_c). Furthermore, the normalized thermal strut loads of both steel and concrete struts decreased as the strut stiffness increased. In Fig. 15, the average of the normalized thermal strut loads is smaller in the concrete strut than in the steel strut. This is because the initial thermal load N_0 is lower in the concrete strut than in the steel strut. In the above context, several factors that affect the computation processes were analyzed, including the structural forms, spacing (vertical and horizontal) and length of struts, overall rigidity of struts, and stiffness of the retained earth (i.e., deformation modulus of soil or coefficient of subgrade reaction).

10. Conclusions

In this paper, based on the Winkler's model, with respect to deep excavation engineering with multilevel struts and by considering soil–structure interactions, a novel approach was developed for calculating the temperature-induced strut loads. The examples showed that the calculation approach is simple and convenient, and the computed results are safe and can be applied to excavation design. Following conclusions can be drawn from the computed results and measured data:

(1) The model developed in this study can shed light on strut–wall–soil interactions. The model shows that the factors influencing the processes include the structural forms, spacing (vertical and horizontal) and length of struts, overall rigidity of strut and stiffness of the retained soil.

(2) The measured results show that the temperature effects have different influences on strut loads at different levels. The influence on strut loads at the lower levels is higher than that at the upper levels. The model proposed in this paper exactly reflects and interprets this situation.

(3) The computed results on temperature-induced strut loads obtained using the approach developed in this study are higher than the measured results. The former is slightly conservative and can be somewhat safe when applied to excavation designs.

Acknowledgments

This study was supported by the National Science Foundation of China under Grant No. 41402245, 51678319.

Appendix

For the *n*-th-level strut, the established local coordinate system is shown in Fig. 5. Here, the horizontal subgrade reaction coefficient is given as $k_h = m(z + H_n - \frac{h_{n-1}}{2})$, and the wall deformation equation under the local coordinate system can be expressed as follows:

$$y = -\frac{2Y_n}{h_n} z + Y_n + \frac{1}{2} Y_n \frac{h_{n-1}}{h_n} \tag{14}$$

The relationship between Y_n and y_{n-1} becomes:

$$y_{n-1} = Y_n + \frac{Y_n \cdot h_{n-1}}{h_n} \tag{15}$$

The Winkler's model provides the following:

$$Q = \int_0^{h_n + h_{n-1}/2} m(z + H_n - \frac{h_{n-1}}{2}) \left[-\frac{2Y_n}{h_n} z + Y_n + \frac{1}{2} Y_n \frac{h_{n-1}}{h_n} \right] \mathrm{d}z \tag{16}$$

Let $N_n^T = D \times Q$; by integrating Eq. (13), the following can be obtained:

$$N_n^T = \frac{1}{24} \frac{mDY_n (h_{n-1} + h_n)^2 (h_n - 2h_{n-1} + 6H_n)}{h_n} \tag{17}$$

Eq. (17) can be rewritten as follows:

$$Y_n = \frac{24 N_n^T h_n}{mD(h_{n-1} + h_n)^2 (h_n - 2h_{n-1} + 6H_n)} \tag{18}$$

REFERENCES

Arboleda-Monsalve, L.G., 2014. Performance,Instrumentation and Numerical Simulation of One Museum Park West Excavation. Ph.D. thesis,Northwestern University.

Batten, M., Powrie, W., Boorman, R., Yu, H., Leiper, Q., 1999. Use of vibrating wire strain gauges to measure loads in tubular steel props supporting deep retaining walls. Proc. Inst. Civ. Eng. - Geotech. Eng. 137, 3–13. https://doi.org/10.1680/gt.1999.370102

Beer, F.P., Johnston, E.R., DeWolf, J.T., Mazurek, D.F., 2012. Mechanics of Materials, 6th Edition, Sixth. ed. McGraw-Hill, New York.

Bono, N.A., Liu, T. k, Soydemir, C., 1992. Performance of an internally braced slurry-diaphragm wall for excavation support, in: American Society for Testing and Materials. ASTM, Philadelphia, pp. 347–360.

Boone, S.J., Crawford, A.M., 2000. Braced excavations: temperature, elastic modulus, and strut loads. J. Geotech. Geoenvironmental Eng. 126, 870–881. https://doi.org/10.1061/(ASCE)1090-0241(2000)126:10(870)

CCEMS, 1997. Technical code for excavation engineering in Shanghai. China, Shanghai. (in Chinese)

Chambers, P., Augarde, C., Reed, S., Dobbins, A., 2016. Temporary propping at Crossrail Paddington station. Geotech. Res. 3, 3–16. https://doi.org/10.1680/jgere.15.00009

Chapman, K.R., Cording, E.J., Schnabel, H., 1972. Performance of a braced excavation in granular and cohesive soils, in: Performance of Earth and Earth-Supported Structures. Purdue University, New York, pp. 271–293.

Endo, M., Kawasaki, T., 1963. Study of thermal stresses acting on struts. Trans. Archit. Inst. Japan 689–692.

Gaba, A.R., Simpson, B., Powrie, W., Beadman, D.R., 2003. Embedded retaining walls: guidance for economic design. London,UK.

Hashash, Y.M.A., Marulanda, C., Kershaw, K.A., Cording, E.J., Druss, D.L., Bobrow, D.J., Das, P.K., 2003. Temperature Correction and Strut Loads in Central Artery Excavations. J. Geotech. Geoenvironmental Eng. 129, 495–505. https://doi.org/10.1061/(ASCE)1090-0241(2003)129:6(495)

He, W., Luo, C., Cui, J., Zhang, J., 2017. Computers and Geotechnics An axisymmetric BNEF method of circular excavations taking into account soil-structure interactions. Comput. Geotech. 90, 155–163. https://doi.org/10.1016/j.compgeo.2017.06.001

Huang, M., Zhang, C., Li, Z., 2009. A simplified analysis method for the influence of tunneling on grouped piles. Tunn. Undergr. Sp. Technol. 24, 410–422. https://doi.org/10.1016/j.tust.2008.11.005

Kumagai, T., Ariizumi, K., Kashiwagi, A., 1999. Behaviour and analysis of a large-scale cylindrical earth retaining structure. Soils Found. 39, 13–26. https://doi.org/10.3208/sandf.39.3_13

Li, L., Xu, Z., Yuan, Y., 2009. Incremental computing of supporting excavation with cover-cut. Proc. Inst. Civ. Eng. - Munic. Eng. 162, 95–102. https://doi.org/10.1680/muen.2009.162

Midas Information Technology Co., Ltd., 2002. GTS Analysis Reference Manual (GTS Version 260). Seol.

Mindlin, R.D., 1936. Force at a point in the interior of a semi-infinite solid. J. Appl. Phys. 7, 195–202. https://doi.org/10.1063/1.1745385

Mu, L., Huang, M., Finno, R.J., 2012. Tunnelling effects on lateral behavior of pile rafts in layered soil. Tunn. Undergr. Sp. Technol. 28, 192–201. https://doi.org/10.1016/j.tust.2011.10.010

Osborne, N.H., Chen, D.C., Ng, C.C., Rudi, J., Latt, K.M., Tan, G.H., 2007. Factors Influencing the Performance of Strain Gauges: A Singapore Perspective, in: Jerry DiMaggio, P.E.. and P.O. (Ed.), Seventh International Symposium on Field Measurements in Geomechanics. ASCE, boston, Massachusetts, United States. https://doi.org/10.1061/40940(307)76

Ou, C., 2006. Deep Excavation: Theory and Practice. Taylor & Francis, London,UK.

Poulos, H.G., Davis, H.E., 1980. Pile Foundation Analysis and Design. New York: John Wiley and Sons.

Powrie, W., Batten, M., 2000. Comparison of measured and calculated temporary-prop loads at Canada Water Station. Geotechnique 50, 127–140. https://doi.org/10.1680/geot.2000.50.2.127

Richards, D.J., Holmes, G., Beadman, D.R., 1999. Measurement of temporary prop loads at Mayfair car park. Proc. Inst. Civ. Eng. - Geotech. Eng. 137, 165–174. https://doi.org/10.1680/gt.1999.370305

Terzaghi, K., Peck, R.B., Mesri, G., 1996. Soil mechanics in engineering practice, 3rd ed. John Wiley and Sons, New York.

Twine, D., Roscoe, H., 1997. Prop loads guidance on design. London. CIRIA Core Programme Funders' Report FR/CP/48. London: Construction Industry Research and Information Association.

Vesic, A.B., 1961. Bending of Beams Resting on Isotropic Elastic Solid. J. Eng. Mech. Div. 87, 1961.

Xiao, H.B., Tang, J., Li, Q.S., Luo, Q.Z., 2003. Analysis of multi-braced earth retaining structures. Proc. Inst. Civ. Eng. - Struct. Build. 156, 307–318. https://doi.org/10.1680/stbu.2003.156.3.307

Zhang, Z.P., Yao, X.Q., 2005. Accident Analysis and Technology Dispose of Certain Deep Foundation Pit. Constr. Technol. 34, 72–73.(in Chinese)

List of Tables

List of figures

Table 1. Comparison of computed results from case 1 among different approaches

Approaches	Computed value (kN)	The degree of restraint(%)	Note
Boone and Crawford	216	29	1st-level strut $I_c = 1.5$
	220	30	2nd-level strut $I_c = 1.5$
	256	35	$I_c = 1.2$
	334	45	$I_c = 0.77$
Chapman et al.	634	86	$E_s = 137$ MPa
	381	52	$E_s = 24$ MPa
Proposed approach	403	55	1st-level strut
	480	65	2nd-level strut
Measured value	**300**	41	1st-level strut
	350	47	2nd-level strut

Table 2. Comparison of computed results from case 2 among different approaches

<table>
<tr><th rowspan="2">Approaches / Strut</th><th colspan="2">Chapman et al.</th><th colspan="2">Boone and Crawford</th><th colspan="2">Proposed approach</th><th>Measured value</th></tr>
<tr><th>Thermal loads/kN/℃</th><th>Degree of restraint</th><th>Thermal loads/kN/℃</th><th>Degree of restraint</th><th>Thermal loads/kN/℃</th><th>Degree of restraint</th><th>Degree of restraint</th></tr>
<tr><td>1st-level strut</td><td rowspan="2">70</td><td rowspan="2">66%</td><td>57</td><td>54%</td><td>56</td><td>53%</td><td>52%</td></tr>
<tr><td>2nd-level strut</td><td>53</td><td>50%</td><td>82</td><td>77%</td><td>63%</td></tr>
</table>

Note: the initial thermal loads per centigrade is about 106.4 kN.

Table 3. Comparison of numerical results and other empirical approaches

E_s (MPa)	Strut	Finite element approach			Proposed approach	Boone and Crawford	Chapman
		Strut load after excavation (kN)	Strut load (ΔT=20°C) (kN)	N_i^T (kN)			
26	1st	61.3	62.3	1	10	51	110
	2nd	183.6	201	17.4	51	62	
60	1st	47.1	52.9	5.8	6	96	172
	2nd	184.6	216.6	32	69	113	
260	1st	40.9	77.8	36.9	68	202	257
	2nd	174.7	267.8	93.1	178	219	

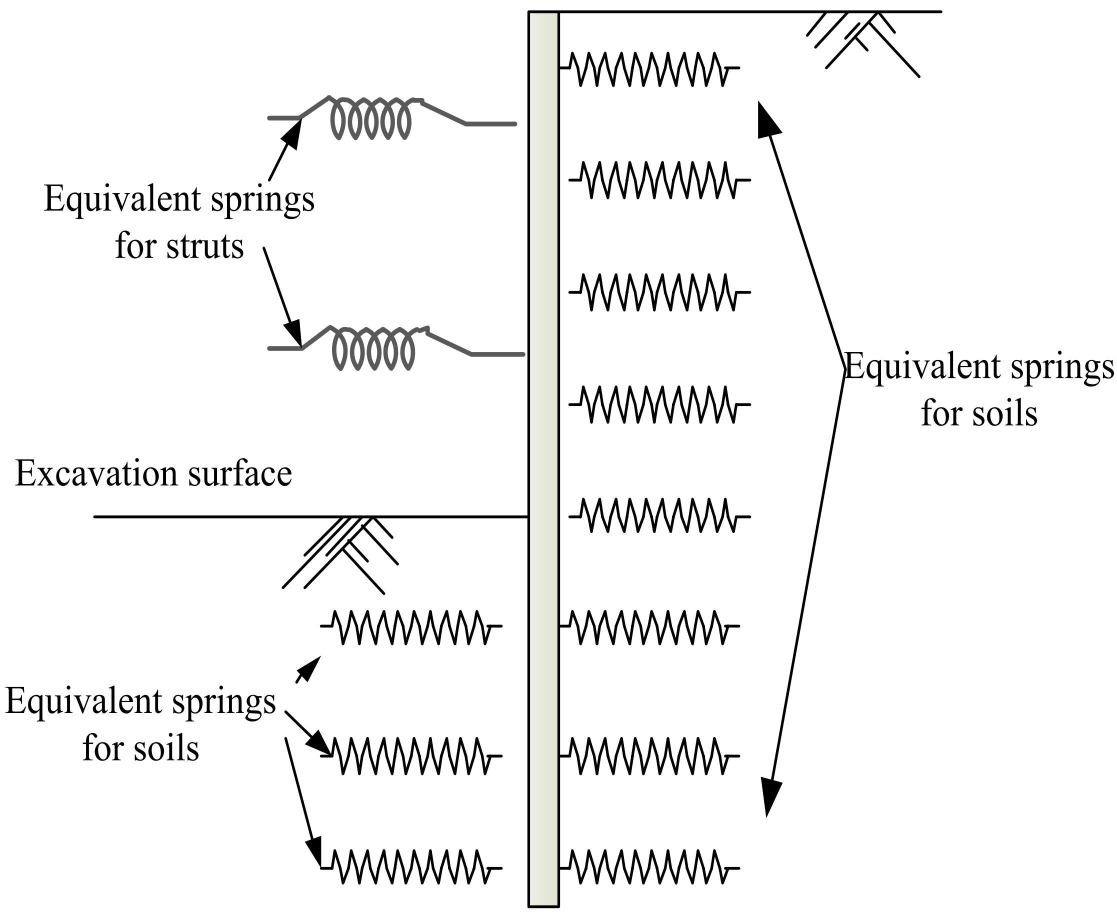

Fig. 1 BEF approach(Ou, 2006)

174×120mm

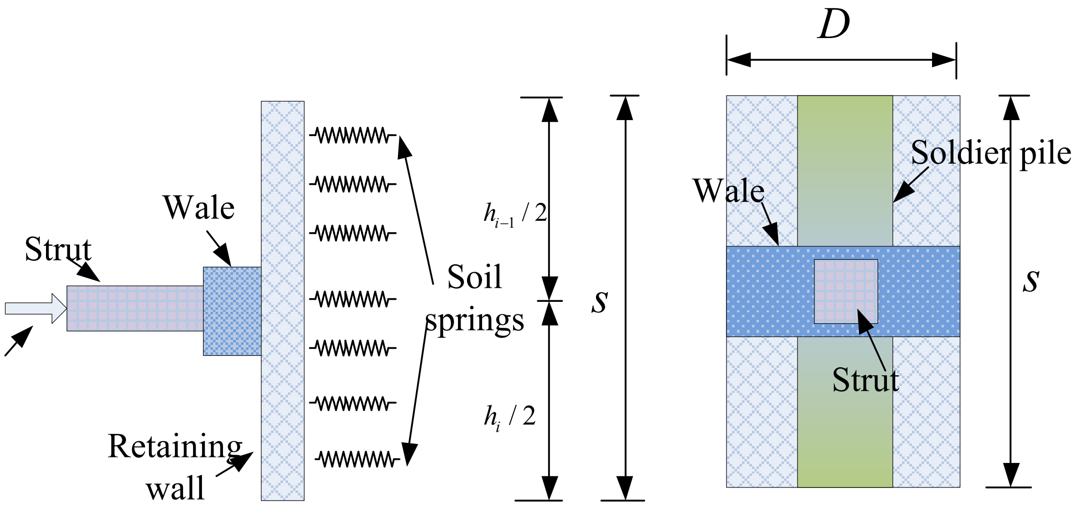

Fig. 2 Model of interactions between struts and soils

129×60mm

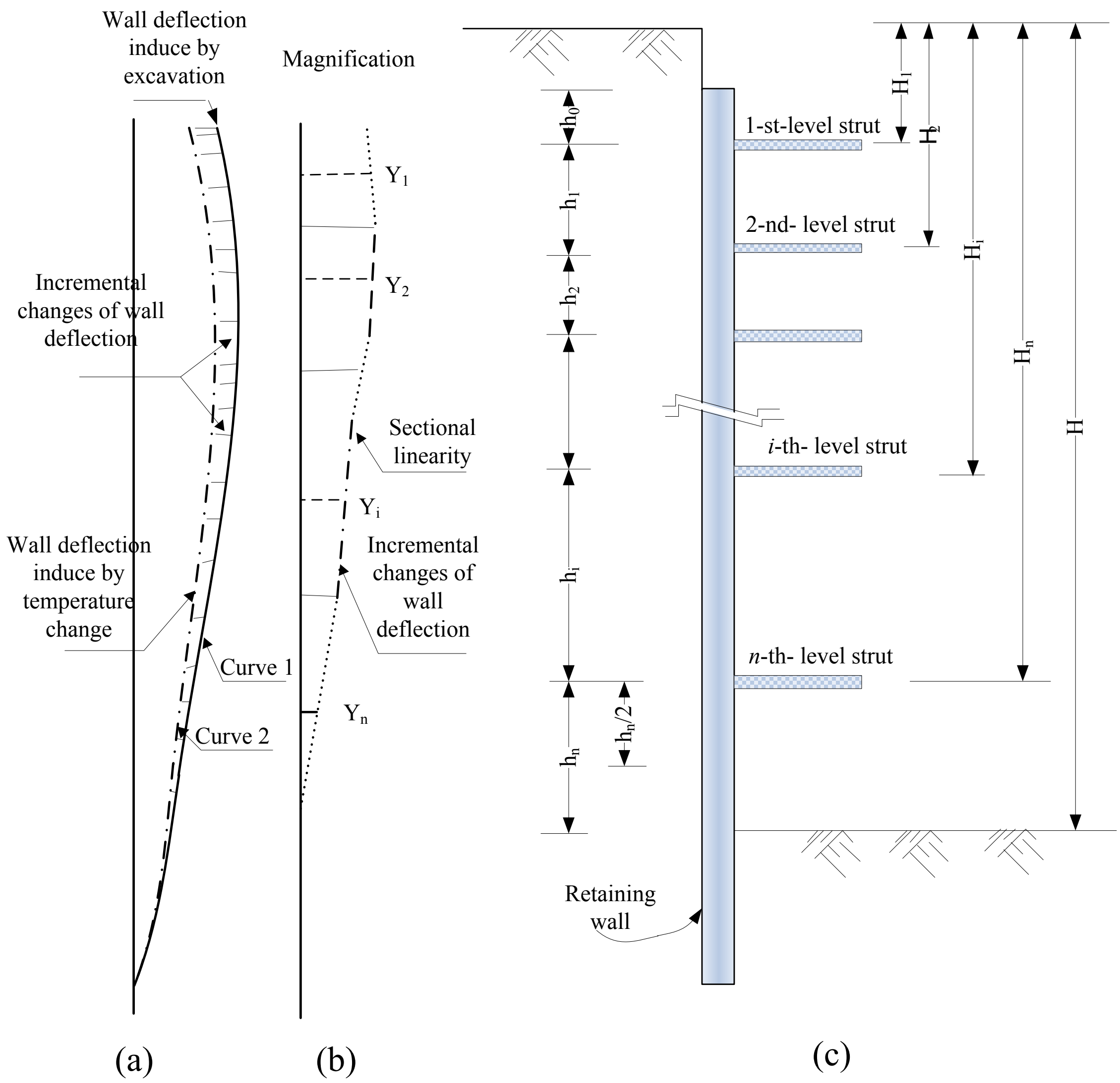

Fig. 3 Simplified model

129× 145mm

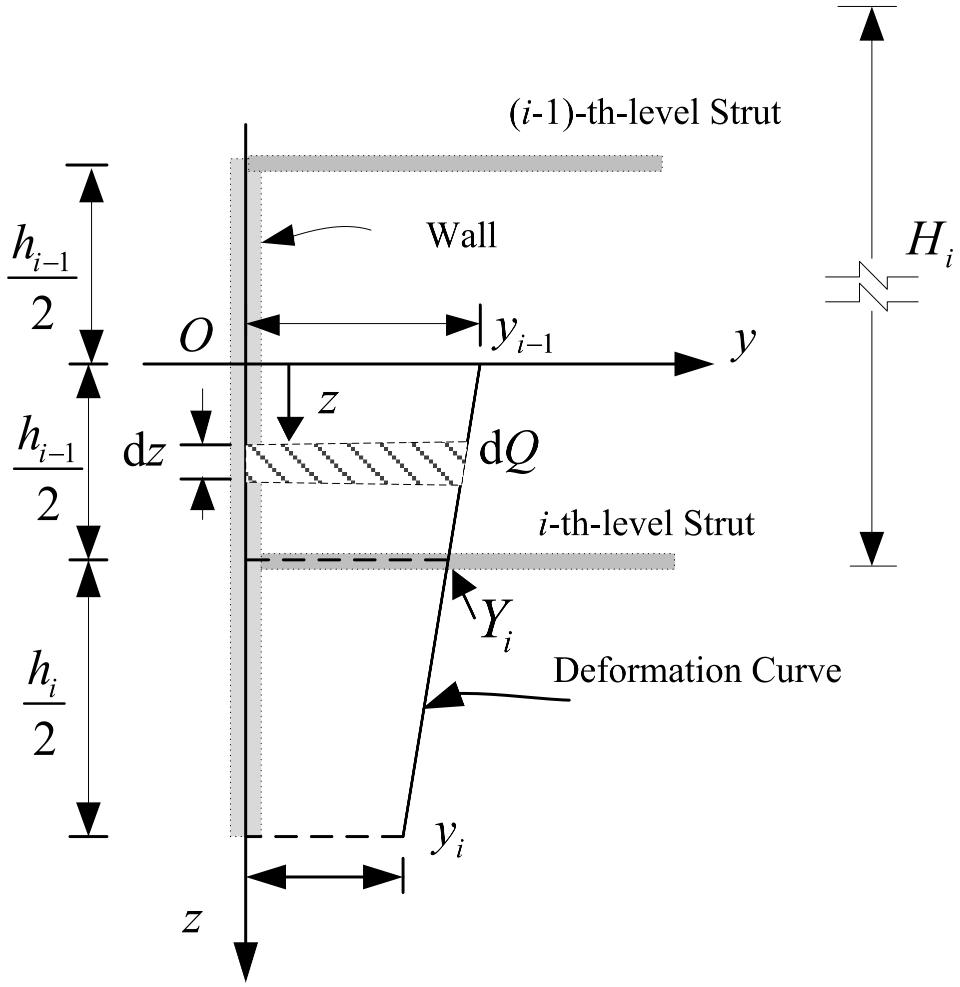

Fig. 4 Coordination of the i-th-level strut

129× 140.8mm

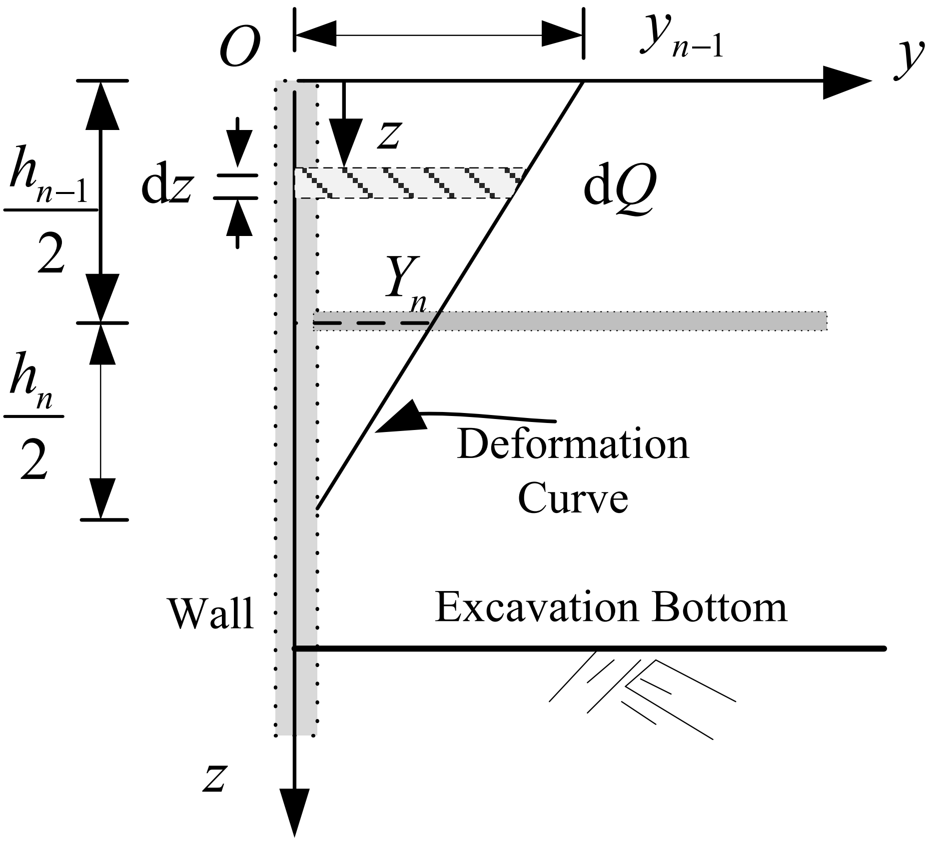

Fig. 5 Coordinate relationship of strut at the *n*-th level

129×122.6mm

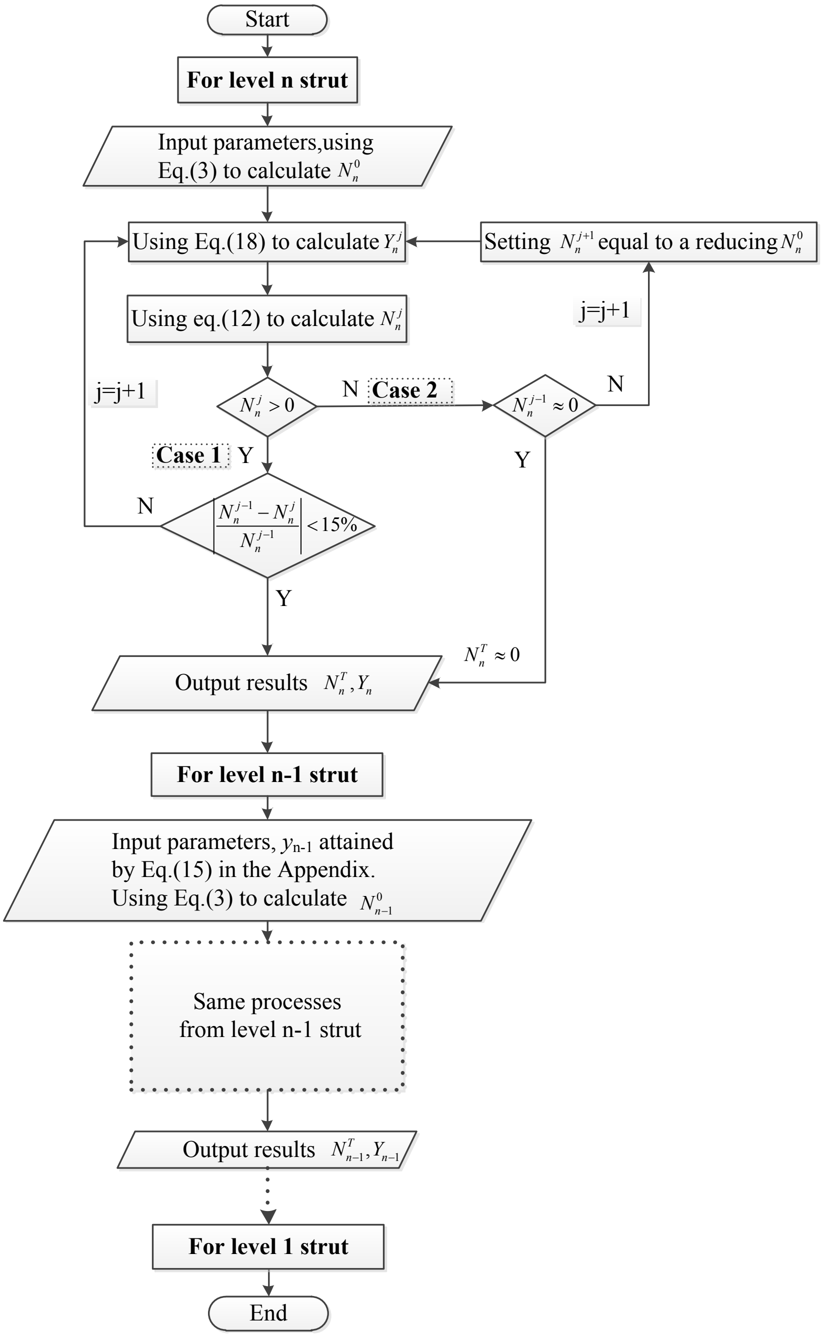

Fig. 6 Flow Chart for computation processes

129×66mm

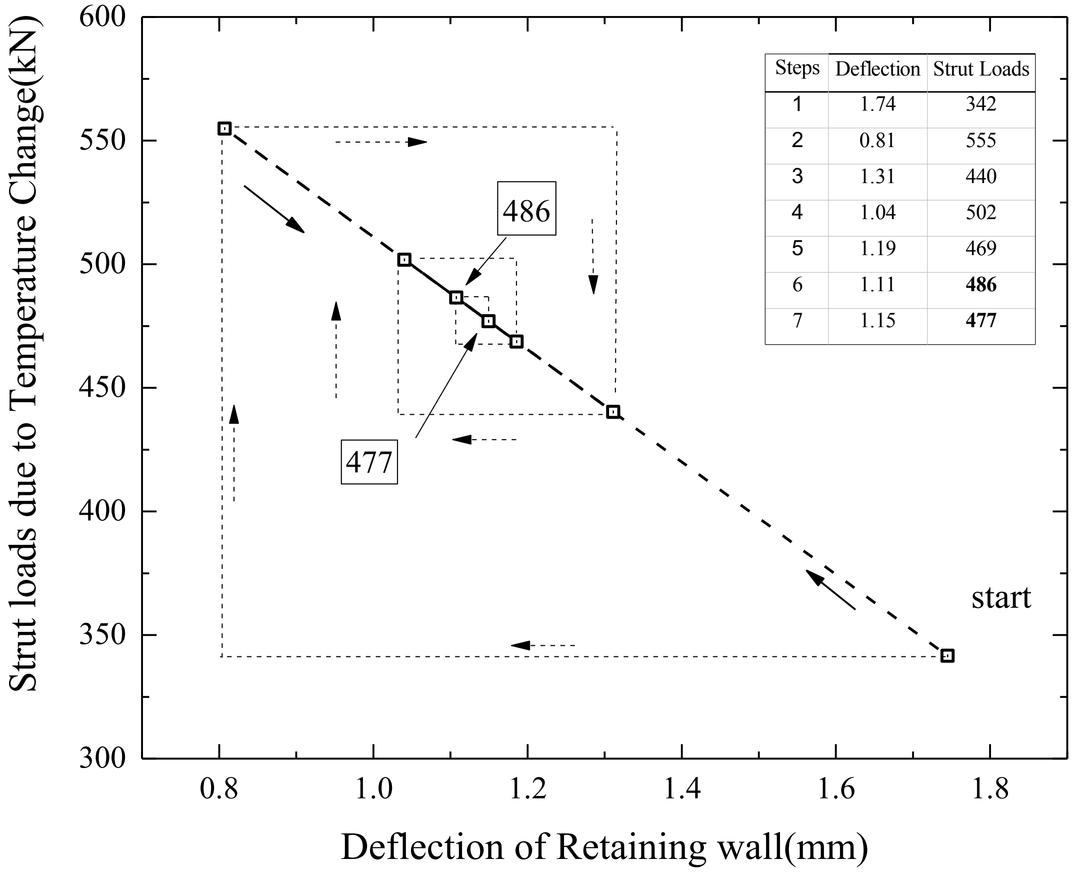

Fig. 7 Computed results of 2nd-level strut

127×150mm

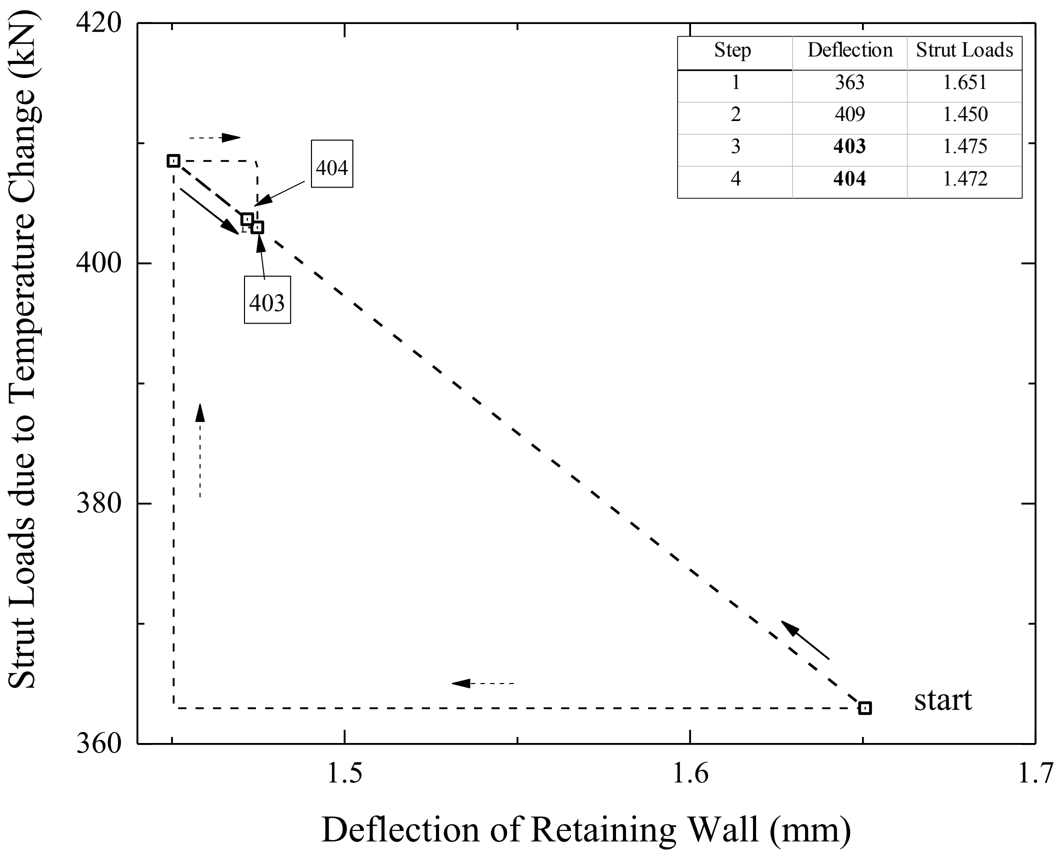

Fig. 8 Computed results of 1st-level strut

116×150mm

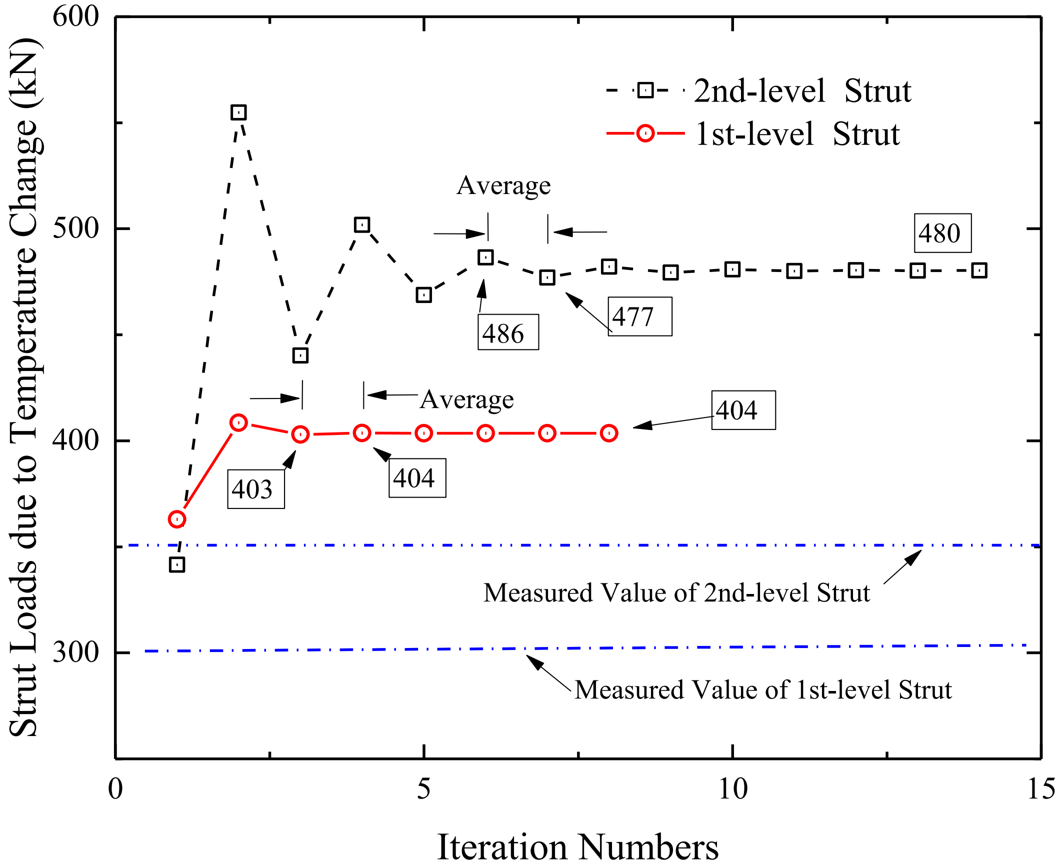

Fig. 9 Iteration procedures of strut loads

116×150mm

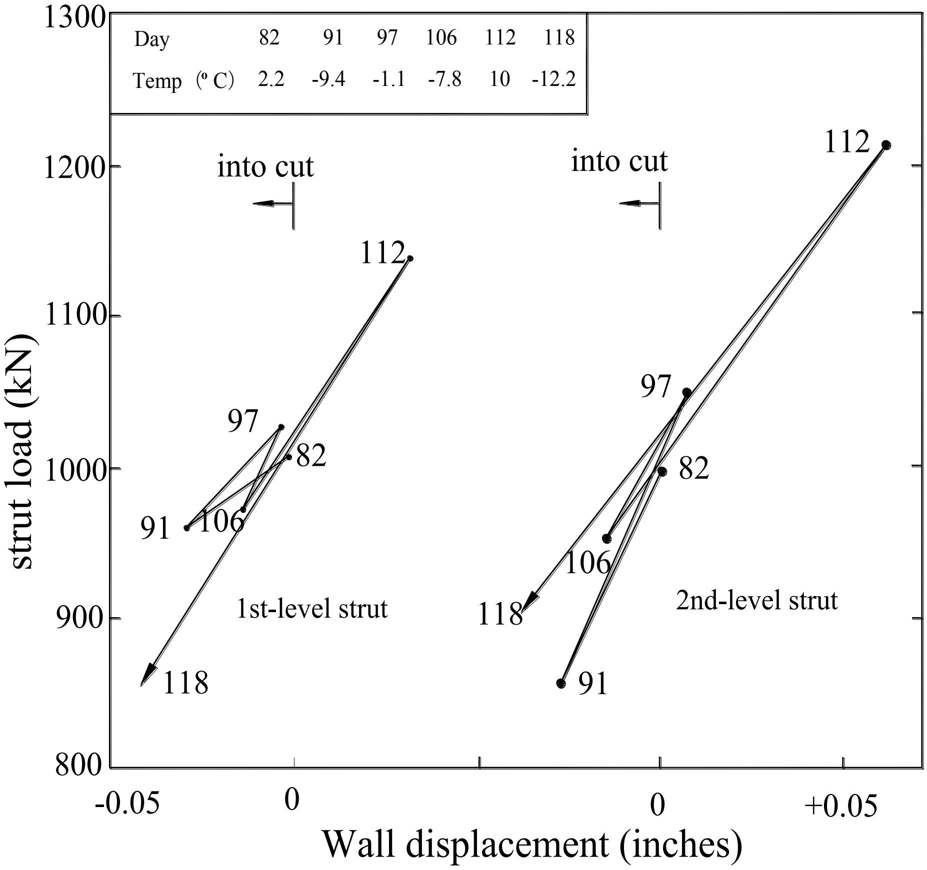

Fig. 10 Strut loads and displacements of wall due to temperature change(Chapman et al., 1972)

12.9×120mm

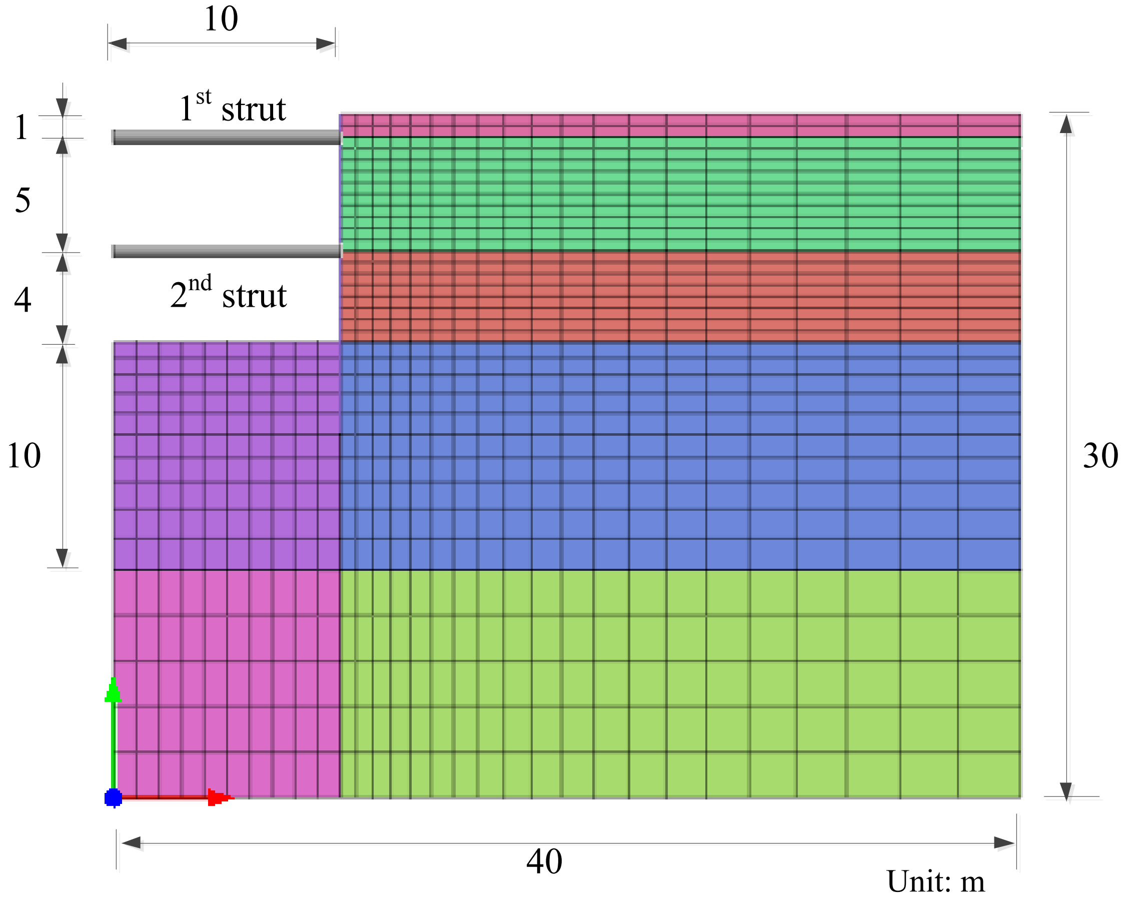

Fig. 11 2-D finite element mesh

150×154mm

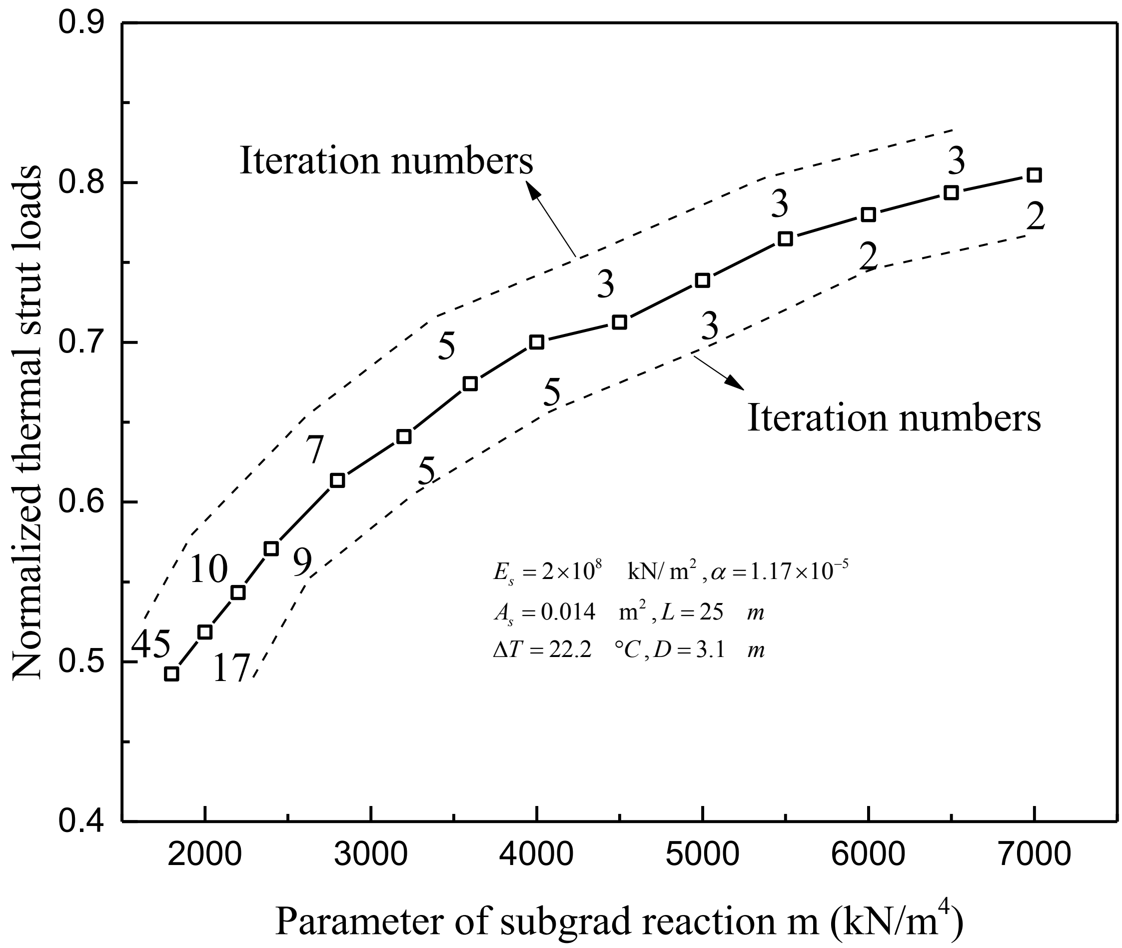

Fig. 12 Relationship between normalized thermal strut loads and soil stiffness

150×154mm

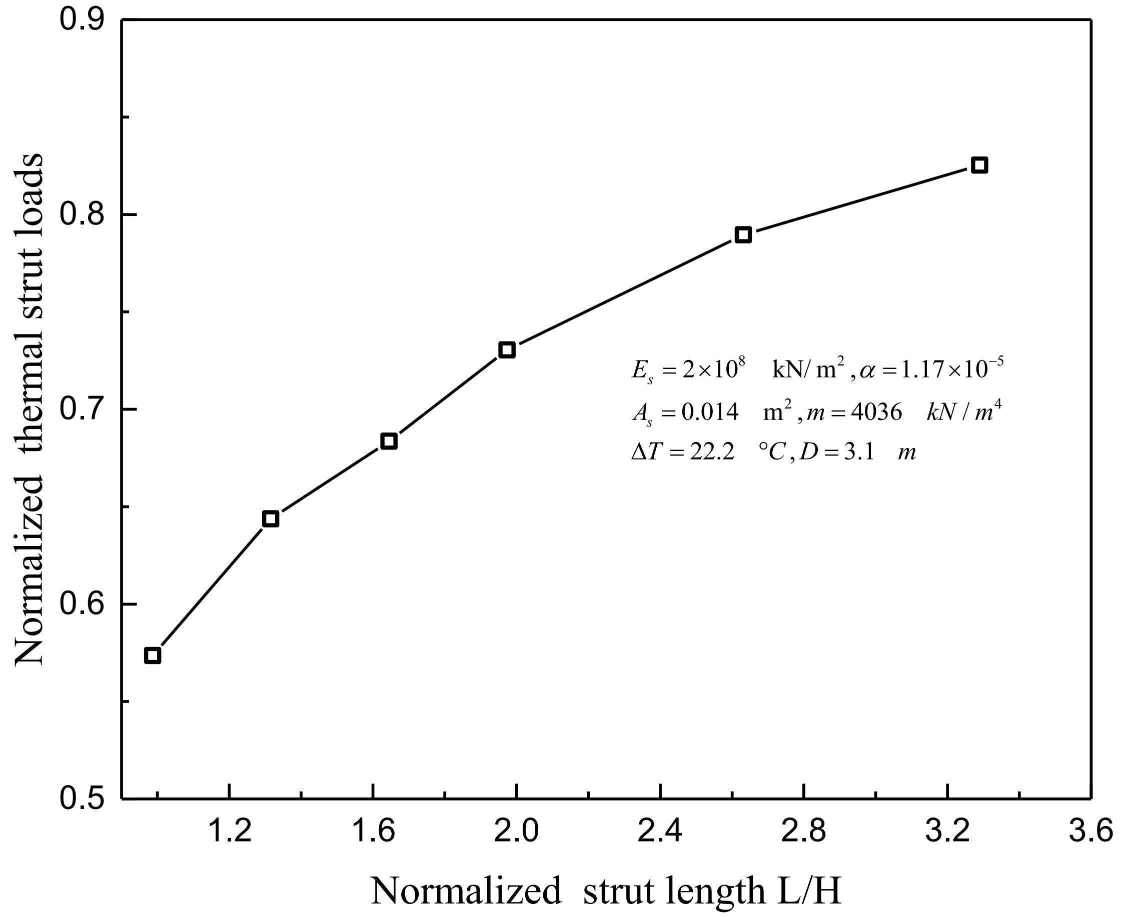

Fig. 13 Relationship between normalized thermal strut loads and strut length

150×154mm

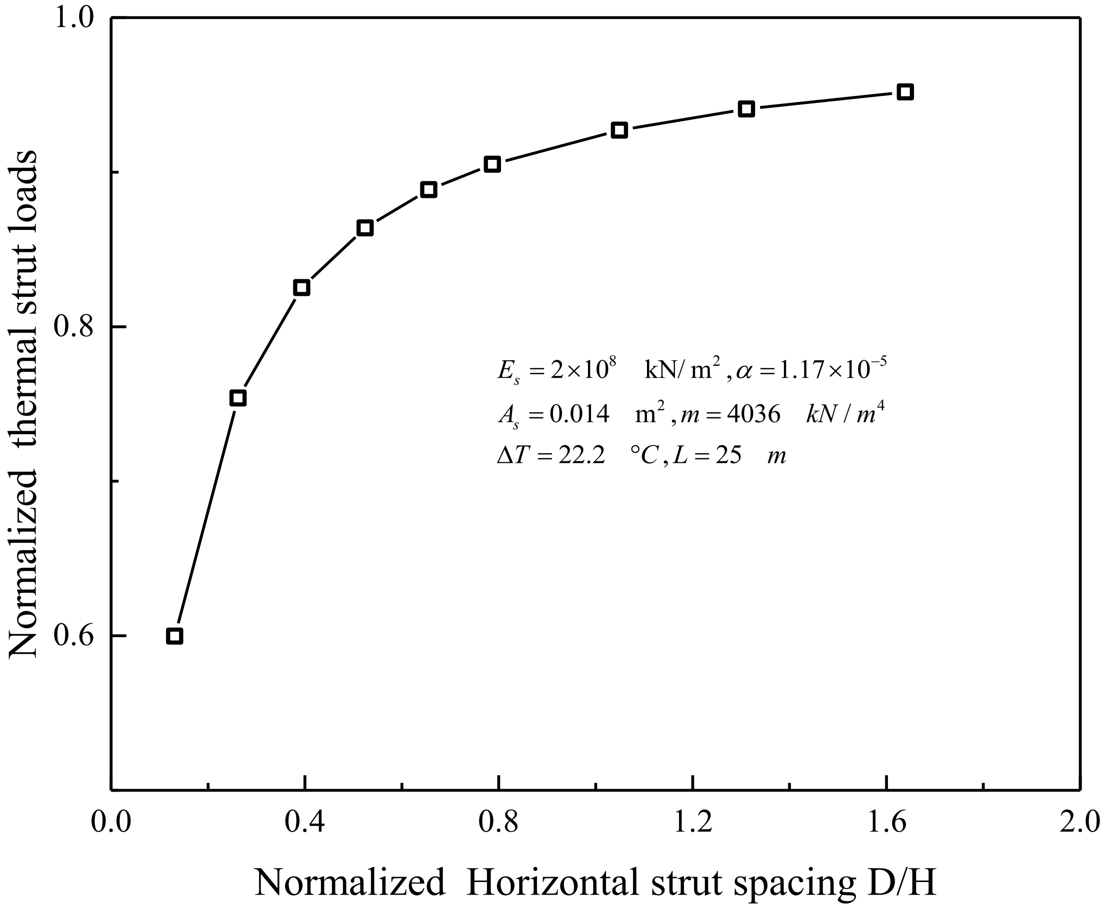

Fig. 14 Relationship between normalized thermal strut loads and horizontal spacing

150×154mm

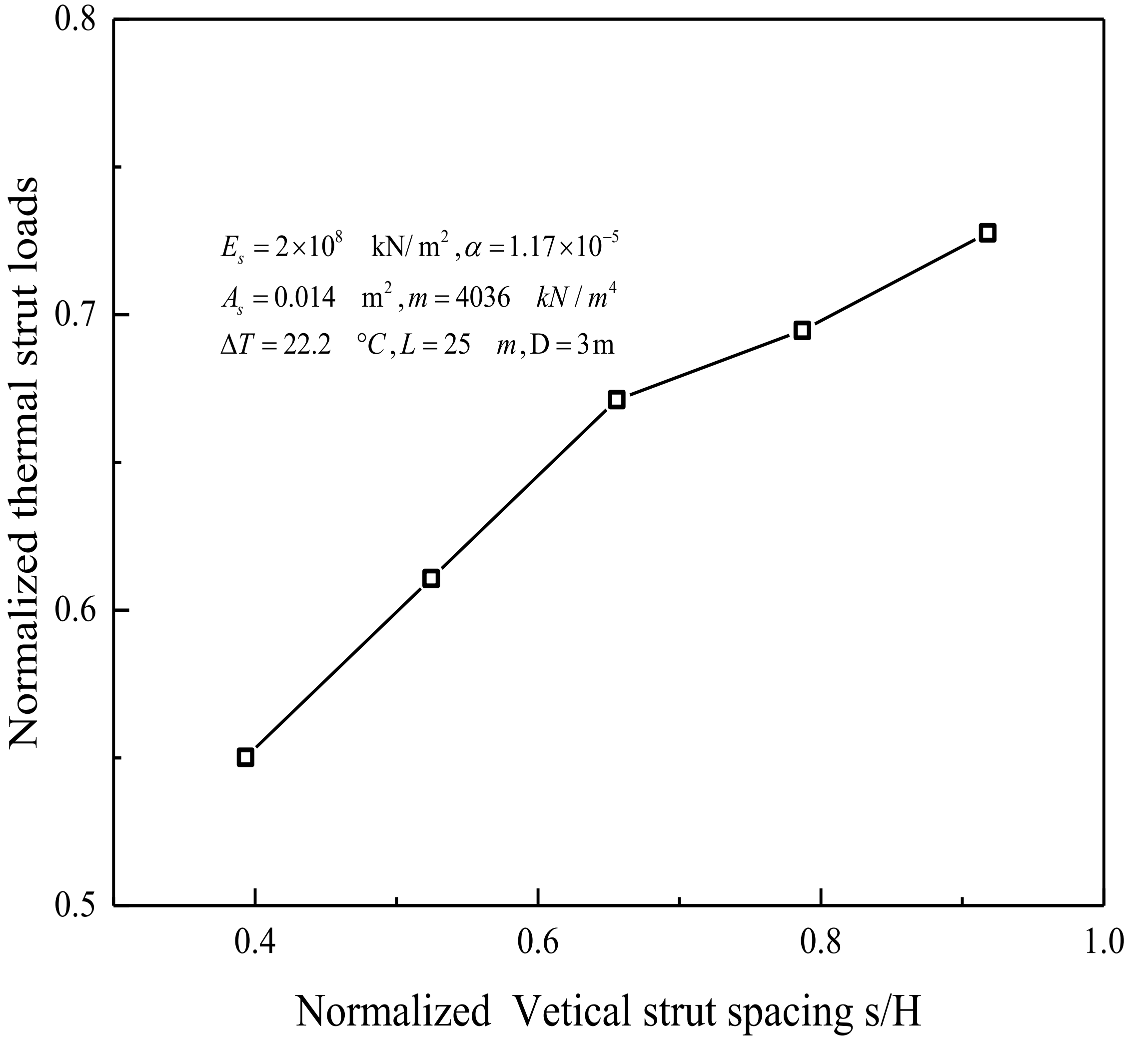

Fig. 15 Relationship between normalized thermal strut loads and vertical spacing

150×154mm

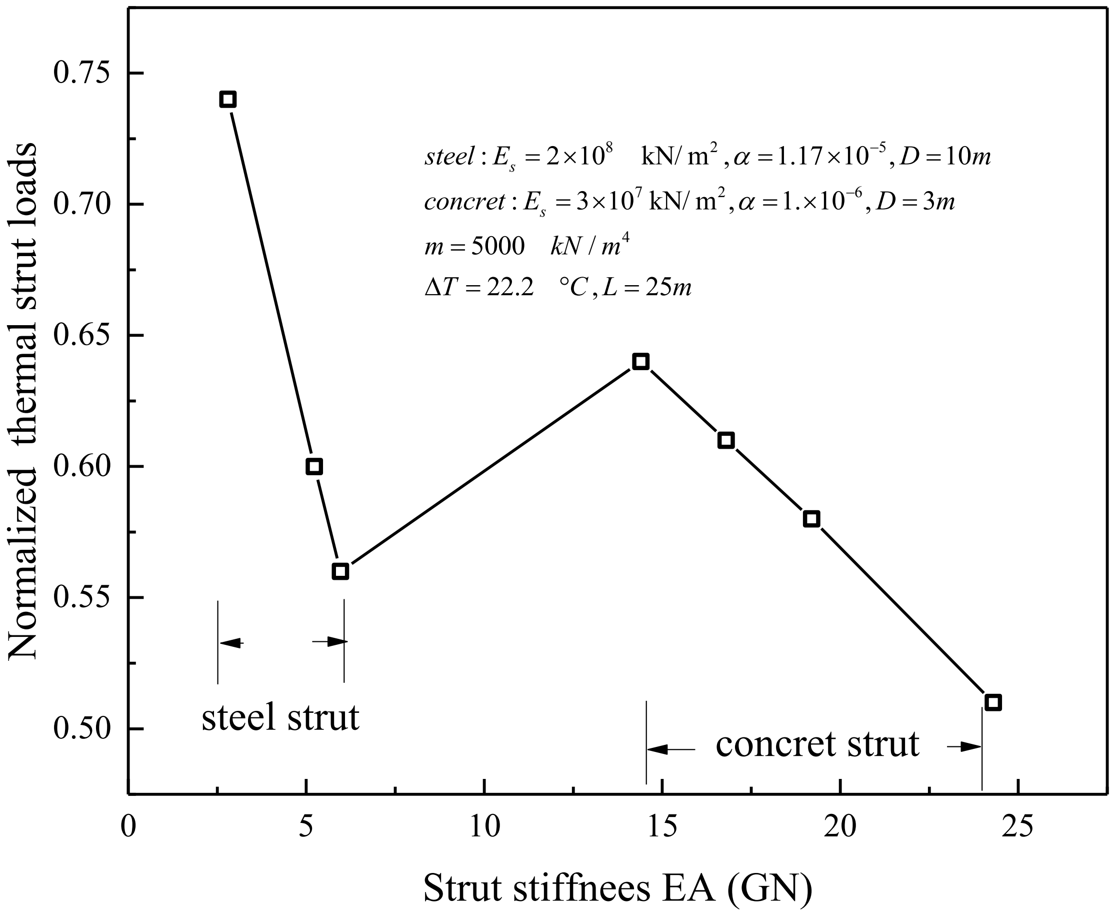

Fig. 16 Relationship between normalized thermal strut loads and strut siffness

150×154mm